Biodegradable Nanoparticles Meet the Bronchial Airway Barrier: How Surface Properties Affect Their Interaction with Mucus and Epithelial Cells

Simona Mura, Hervé Hillaireau, Julien Nicolas, Saadia Kerdine-Römer, Benjamin Le Droumaguet, Claudine Deloménie, Valérie Nicolas, Marc Pallardy, Nicolas Tsapis, Elias Fattal

Biodegradable nanoparticles meet the bronchial airway barrier: how surface properties affect their interaction with mucus and epithelial cells

Simona Mura,[§] *Hervé Hillaireau,*[§] *Julien Nicolas,*[§] *Saadia Kerdine-Römer,*[ς] *Benjamin Le Droumaguet,*[§] *Claudine Deloménie,*[†] *Valérie Nicolas,*[‡] *Marc Pallardy,*[ς] *Nicolas Tsapis,*[§] *Elias Fattal,*[§,*]

[§] Univ. Paris-Sud, Laboratoire de Physico-Chimie, Pharmacotechnie et Biopharmacie, UMR CNRS 8612, Faculté de Pharmacie, 5 rue Jean-Baptiste Clément, F-92296 Châtenay Malabry cedex, France

[ς] Univ. Paris-Sud, INSERM UMR996, Cytokines, Chimiokines et immunopathologie, 5 rue Jean-Baptiste Clément, F-92296 Châtenay-Malabry cedex, France

[†] IFR IPSIT (Institut Paris-Sud d'Innovation Thérapeutique) TRANS-PROT, 5 rue Jean-Baptiste Clément, F-92296 Châtenay-Malabry cedex, France

[‡] IFR IPSIT (Institut Paris-Sud d'Innovation Thérapeutique) Imagerie Cellulaire 5 rue Jean-Baptiste Clément, F-92296 Châtenay-Malabry cedex, France

[*]To whom correspondence should be addressed.

E-mail: elias.fattal@u-psud.fr Tel: +33 1 46 83 55 82 Fax: +33 1 46 83 59 46

ABSTRACT

Despite the wide interest raised by lung administration of nanoparticles (NPs) for the treatment of various diseases, little information is available on their effect towards the airway epithelial barrier function. In this study, the potential damage of the pulmonary epithelium upon exposure to poly(lactide-*co*-glycolide) (PLGA) NPs has been assessed *in vitro* using a Calu-3-based model of the bronchial epithelial barrier. Positively and negatively charged as well as neutral PLGA NPs were obtained by coating their surface with chitosan (CS), poloxamer (PF68) or poly(vinyl alcohol) (PVA), respectively. The role of NP surface chemistry and charge on the epithelial resistance and mucus turnover, using MUC5AC as a marker, was investigated. The interaction with mucin reduced the penetration of CS- and PVA-coated NPs while the hydrophilic PF68-coated NPs diffused across the mucus barrier leading to a higher intracellular accumulation. Only CS-coated NPs caused a transient but reversible decrease of the trans-epithelial electrical resistance (TEER). None of the NPs formulations increased MUC5AC mRNA expression or the protein levels. These *in vitro* results highlight the safety PLGA NPs towards the integrity and function of the bronchial airway barrier and demonstrate the crucial role of NPs surface properties to achieve a controlled and sustained delivery of drugs *via* the pulmonary route.

KEYWORDS

Nanoparticles, PLGA, surface properties, Calu-3, bronchial airway barrier, trans-epithelial electrical resistance, mucus

INTRODUCTION

Biomedical applications of nanotechnologies have raised many hopes for improving the treatment and diagnosis of severe pathologies [1-3]. Indeed, the administration of drug-loaded nanomedicines can not only improve the therapeutic efficiency but also reduce the side effects and toxicity of the parent drug. Nanoscaled polymeric nanoparticles (NPs) have been used for controlled and targeted delivery of drugs *via* different routes of administration. Among them, the delivery to the lung gave rise to a large interest during the past decade. This non invasive route of administration is attractive for both local treatment of lung diseases and systemic drug absorption [3-5]. Pulmonary drug delivery offers several advantages: a large epithelial surface for absorption [6], high blood flow, weak enzymatic activity and avoidance of the first pass metabolism. Moreover, after lung administration, NPs are well retained *in situ* and weakly taken up by macrophages providing their diameter is lower than 260 nm [7].

After inhalation, the first interface encountered by NPs is constituted by the epithelial cells which line the airway compartment. These cells form a physical barrier which represents the first defense against inhaled exogenous pathogens and harmful materials. The barrier function of the airway epithelium is dependent on physical interactions between adjacent cells, mainly mediated by tight junctions [8] whose role is to ensure an impermeable layer to exogenous materials [9-12]. Moreover, in the large airways, a continuously renewed mucus layer constitutes another efficient barrier to assure the defense against inhaled materials [13-14]. Mucus is mainly composed of water and mucins which are long, flexible, highly glycosilated proteins that represent around 1-5 % of the total mucus weight [15-16]. Mucus traps the inhaled materials which are then effectively removed from the respiratory tract toward the upper end of the tracheal tube *via* the muco-ciliary clearance process [16]. Upon entering the pharyngeal region, NPs are swallowed and undergo further processing in the gastrointestinal tract [17]. This complex mechanism which guarantees lung integrity in physiological conditions can undergo important changes when associated to pathological diseases or to the inhalation of various toxic compounds. Indeed, chronic disorders of the inflammatory tract, such as asthma and cystic fibrosis as

well as exposure to cigarette smoke, pollutants and urban particular matter are associated to impaired barrier function and changes in the composition of mucus layer [18-23]. The increased permeability of epithelium and the mucus hypersecretion contribute to airway obstruction, which facilitates bacterial infection, lung inflammation and eventually a decline of the pulmonary function [16]. To achieve a targeted and controlled delivery of drugs to the lung, NPs must be able to overcome these physiological barriers. The mucus layer is the first obstacle to NP diffusion and cellular uptake, which means that administered NPs could be efficiently entrapped within the mucin network and quickly removed. Nevertheless, it has been observed that surface properties influence NP's ability to interact with and rapidly diffuse through the mucus barrier, offering the possibility to target the underlying cells [24-26].

Whether this process may cause any damage to the airway epithelium altering the integrity of the epithelial barrier and the muco-ciliary mechanism is an important issue. In a previous work [27], we have highlighted the *in vitro* toxicity of biodegradable NPs on a Calu-3-based model of bronchial epithelium, by demonstrating that NPs did not cause important cytotoxicity or inflammatory cytokines release regardless of their surface properties. The aim of this work was to address the role of NP surface chemistry and surface charge on the *in vitro* potential impairment of the bronchial epithelial barrier. For this purpose, three types of surface-modified NPs were used: positively and negatively charged as well as neutral ones. NPs were formulated using poly(lactide-*co*-glycolide) (PLGA), one of the most commonly used biodegradable and biocompatible polymers involved in the formulation of nanomedicines [28-30]. The Calu-3 cell line cultured at air/liquid interface has been used to mimic the bronchial epithelium barrier [31]. The ability of NPs to diffuse across the mucus layer and their subsequent cellular uptake, as well as their potential effect on the epithelial permeability and the mucus turnover were assessed. Changes in mucus production were quantified using the MUC5AC protein as a marker of mucus secretion. The expression of the corresponding gene was also investigated.

MATERIALS AND METHODS

Chemicals. Poly(lactide-*co*-glycolide) (PLGA) (75:25 Resomer® RG756 and 50:50 Resomer® RG503H) were purchased from Boehringer-Ingelheim (Germany). Poly(vinyl alcohol) (PVA) (87-89 % hydrolyzed, MW 30-70 kDa) and acrolein (≥ 95.0%) were obtained from Sigma Aldrich (France). Mowiol® 4-88 PVA (MW 30 kDa) was a gift from Kuraray Specialities Europe GmbH (Frankfurt, Germany). Ultrapure chitosan chloride (CS, Protasan® UP CL113, 75-90% deacetylation, MW 50-150 kDa) was purchased from NovaMatrix (FMC BioPolymer, Drammen, Norway). Pluronic® F68 (PF68) was obtained from BASF (France). All solvents were provided at the highest grade by Carlo Erba (Italy). Water was purified using a Synergy System (Millipore, France).

Nanoparticle preparation. NPs with different surface properties were prepared by the solvent emulsion evaporation method [32]. Neutral NPs (PLGA/PVA NPs) were obtained by dissolving 100 mg of PLGA into 5 mL of a dichloromethane/acetone (1/1 v/v) mixture. First, this organic solution was pre-emulsified with 20 mL of a 0.25 % (w/v) PVA (MW 30-70 kDa) aqueous solution by using a vortex for 1 minute. The pre-emulsion was kept on ice and sonicated for 1 minute using a VibraCell Sonicator (Fischer Scientific, Illkirch, France) at 40% of power. To prepare positively-charged NPs (PLGA/CS NPs), the organic solution of PLGA was pre-emulsified with a 0.6 % (w/v) aqueous CS solution containing 0.5 % (w/v) of Mowiol® 4-88 PVA using a vortex for 1 minute. This pre-emulsion was kept on ice and sonicated for two min using a VibraCell Sonicator (Fischer Scientific, Illkirch, France) at 40% of power. Then, for both neutral and positively-charged NPs, the organic phase was evaporated at room temperature upon magnetic stirring (600 rpm). NP dispersion was then completed to 20 mL. The excess of stabilizers was removed by centrifugation of the NP suspension at 37000 × *g* for 1 h at 4 °C and the pellet containing the NPs was resuspended in ultrapure water. Negatively-charged NPs (PLGA/PF68 NPs) were prepared by using PF68 as stabilizer. In this specific case, PLGA was dissolved in 10 mL of ethyl acetate and added dropwise to 20 mL of a 1 % (w/v) aqueous

solution of PF68 under vigorous magnetic stirring. The pre-emulsion was vortexed for 1 minute and then sonicated for another minute using a VibraCell Sonicator (Fischer Scientific, Illkirch, France) at 40% of power. A constant volume of water (20 mL) was added to the emulsion, in order to promote the diffusion of the organic solvent into the external phase, leading to the formation of NPs. The organic phase was evaporated at room temperature upon magnetic stirring (600 rpm). Rhodamine-tagged NPs were prepared as described above by dissolving a 70/30 (w/w) mixture of PLGA and rhodamine-tagged PLGA (Rhod-PLGA) in the organic solvent. Rhod-PLGA was synthetised as described previously [27].

Nanoparticle characterization. NP average diameter was measured by dynamic light scattering (DLS) with a Nano ZS from Malvern (173° scattering angle) at a temperature of 25 °C. Measurements were performed in triplicate following dilution of the NP suspension in water. The surface charge of NPs was investigated by ζ-potential (mV) measurement at 25 °C, after dilution with 1 mM NaCl, using the Smoluchowski equation. Stability of the fluorescent Rhod-PLGA NPs was assessed as described previously [27].

Calu-3 cell line culture. The Calu-3 cell line was obtained from ATCC (Catalog Number HTB-55) and maintained at 37 °C and 5 % CO_2 in a humidified atmosphere. Cells were cultured in Dulbecco's modified Eagle's medium (DMEM, Lonza, Belgium) supplemented with 50 $U.mL^{-1}$ penicillin, 50 $U.mL^{-1}$ streptomycin and 10 % fetal bovine serum (FBS, Lonza, Belgium). The medium was changed every four days and cells were passed weekly at a 1/3 split *ratio* using Trypsine-Versene (EDTA) (Lonza, Belgium).

Trans-epithelial electrical resistance. To study the epithelial barrier permeability and the cellular uptake, Calu-3 cells were cultured at an air/liquid interface. 500 µL of cell suspension were seeded at a density of 6 x 10^5 $cells.mL^{-1}$ onto clear polyester Transwell® cell culture inserts (1.12 cm^2, 0.4 µm pore size) (CoStar Corning, Corning, UK) and 1.5 mL of medium was placed in the basolateral chamber. Cells were incubated for 24 h, after which the medium was aspirated from the

apical and the basolateral chamber and replaced by fresh medium only in the basolateral compartment. Thereafter, the medium was renewed in the basolateral chamber every two days. Cell layers were used for experiments only after a stable polarised epithelial layer was formed, which occurred after 10 to 14 days of culture. The formation of tight junctions and a confluent monolayer was monitored by measuring the trans-epithelial electrical resistance (TEER) using chopstick electrodes (STX-2) and an EVOM Epithelial Voltohmmeter (World Precision Instruments, Inc, Sarasota, USA). The first measurement of the TEER was performed after seven days of culture on Transwell® inserts, and then every two days. Before each measurement, 500 µL of pre-warmed medium were placed in the apical compartment and cells were incubated at 37 °C for 30 min. TEER values were calculated by subtracting the resistance value of the cell-free culture support from the resistance measured across each cell layer and correcting the value for the surface area of the Tranwell® insert. Measurements were performed in triplicate.

The integrity of the monolayer was assessed by TEER measurements. Only confluent monolayers which shown a TEER value of at least 300 $\Omega.cm^2$ were used to investigate the effect of NPs on epithelial barrier function integrity. Upon starting the experiment (t = 0), the basolateral compartment was filled with 1.5 mL of fresh pre-warmed cell medium and 500 µL of NPs at a 200 $\mu g.mL^{-1}$final concentration were placed on the cell monolayer in the apical chamber. TEER was measured before and after 12 or 24 h incubation. In another set of experiments, when incubating monolayers with PLGA/CS NPs, TEER values were measured at shorter time intervals between 0 and 24 h in order to follow any variation of the epithelial permeability. Monolayers incubated with cell culture medium were used as control. TEER values were expressed relative to the initial (t = 0) value.

Uptake kinetics. For uptake studies, differentiated Calu-3 monolayers grown on Transwell® inserts for 14-17 days (TEER $\geq$ 300 $\Omega.cm^2$) were used. 500 µL of Rhod-PLGA NPs at a 200 $\mu g.mL^{-1}$ final concentration were applied on the cell monolayer. At different time points (4, 8, 12 and 24 h), monolayers were washed and cells were detached from the inserts by incubation with Trypsine/EDTA

for 10 min. The cell dispersion was centrifuged at 100 × *g* for 10 min and the pellet was recovered in appropriate volume of PBS. The amount of Rhod-PLGA NPs taken up by the Calu-3 was measured on a FACSCalibur® cell analyzer (Becton Dickinson). The fluorescence emission was collected in the fluorescence-2 (FL-2) channel. Cellular debris were eliminated from the analysis using a gate on forward and side scatter. For each sample, 10^4 cells were analyzed. Data acquisition and analysis were performed using the software CellQuest Pro Version 4.02 (BD Biosciences). Experiments were performed in triplicate.

Confocal Laser Scanning Microscopy. In order to assess the interaction between NPs and the mucus which covers the confluent monolayers, differentiated Calu-3, grown for 14 to 17 days on Transwell® inserts (TEER ≥ 300 $\Omega.cm^2$), were exposed to Rhod-PLGA NPs at a 200 $\mu g.mL^{-1}$ final concentration for 24 h. Monolayers were then washed with PBS and the mucus layer was stained by incubation with Alexa Fluor® 488-labeled wheat germ agglutinin (10 $\mu g.mL^{-1}$) (Invitrogen, Molecular Probes®, France) for 10 min at 37°C. After a washing step with PBS, the cell layer-supporting membranes of the Transwell® inserts were cut from the plastic support, mounted on microscopes slides and covered with cover slips. Slides were immediately visualized under a Leica TCS-SP2 spectral confocal laser scanning microscope (Leica Microsystems). Alexa Fluor® 488 and rhodamine were excited with the 488-nm argon laser line and 543-nanometer helium neon laser line, respectively. Image visualization and processing was performed using IMARIS software (Bitplane AG, Zurich, Switzerland).

MUC5AC protein production. Differentiated Calu-3 monolayers grown on Transwell® inserts for 14-17 days (TEER ≥ 300 $\Omega.cm^2$) were incubated with 500 µL of each PLGA NP suspension at a 200 $\mu g.mL^{-1}$ final concentration. At different time points, the incubation medium was withdrawn and the cell layer was washed by incubation with 500 µL of PBS at 37 °C for 30 min. The washing step was repeated three times to remove the whole mucus layer. Cells were then detached from the permeable support and centrifuged at 8609 × *g* for 5 min. 200 µL of lysis buffer (50 mM

HEPES buffer, 150 mM NaCl, 10% glycerol, 1% Triton, 1.5 mM $MgCl_2$, 1mM EGTA) were added to each pellet. As a positive control, cell exposed to 0.05 mM acrolein were used (sensitivity of Calu-3 cells to acrolein was assessed beforehand by an MTT assay, ensuring at least 90% viability at this concentration). Incubation medium, washing solutions and cell lysates were stored separately and kept at −80°C until use. To quantify the amount of MUC5AC protein in the washing solutions and in the cell lysates, a commercial ELISA kit was used following the indications of the manufacturer (CUSABIO BIOTECH CO., Ltd). The total amount of protein contained in each sample was then quantified using the Bradford assay. Experiments were performed in triplicate.

MUC5AC gene expression. Confluent monolayers grown onto T25 flasks were incubated with the three types of PLGA NPs at a 200 $\mu g.mL^{-1}$ final concentration. At different time points (4, 8, 12, 24 and 48 h), the incubation medium was withdrawn and cells were covered with 2 mL of TRIzol® reagent (Invitrogen, Cergy Pontoise, France). Untreated cells and 0.05 mM acrolein-treated cells were used as negative and positive control respectively. Cells were kept at −80°C until RNA extraction.

Total RNA was extracted from the Calu-3 cells with TRIzol® reagent according to the manufacturer's instructions. RNA concentration was measured by reading the absorbance at 260 nm using a Biomate 3 spectrophotometer (Thermo Fisher Scientific, Illkirch, France). Quality control of total RNA was performed by the Bioanalyzer 2100 technology (Agilent Technologies). First-strand cDNA was synthesized from 1 µg of total RNA with 10 $ng.\mu L^{-1}$ random primers (Fermentas, Germany) and 10 $U.\mu L^{-1}$ RevertAid® Premium Reverse Transcriptase (Fermentas, Germany), in a final volume of 20 µL. Quantitative PCR (qPCR) was performed in a CFX96™ Real-Time thermal cycler (Bio-Rad). Two reference genes (HPRT1 and RPLPO) were selected using the geNorm algorithm [33] and were subsequently used to normalize target gene expression levels. The primer sequences of reference and target genes are reported in Table 1. A 50-fold dilution of each cDNA was amplified in duplicate in 10-µl reactions, using the SsoFast™ EvaGreen® Supermix reagent (Bio-

Rad), in the presence of primers at a 500-nM final concentration for each. The qPCR protocol entailed a 30-seconds initial denaturation at 95°C, followed by 45 cycles of the following 2 steps: 2 seconds of denaturation at 95°C and 5 seconds of annealing-extension at 60°C. The amplification specificity was checked by melting curve analysis and agarose gel electrophoresis of PCR products. For each primer pair, the negative controls (i.e. no-template or no-reverse transcriptase controls) produced no amplification signal, suggesting that primer dimerization and genomic DNA contamination were negligible. The Cq values were calculated using the regression algorithm. Standard curves were established for each gene from serial dilutions of the cDNA from control cells. All PCR efficiencies (E) calculated from the slopes of the calibration curves according to the equation $E = [10^{-1/k}] - 1$ (k = slope of the standard curve) were above 90%. The transcripts of reference genes were quantified in each cDNA to normalize for sample-to-sample differences in RNA concentration, quality or reverse transcription efficiency. The target transcript levels were calculated relative to control (untreated) cells, leading to gene expression values in arbitrary units (A.U.).

Statistical analysis. The differences between cells exposed to NPs or the positive control and untreated cells were evaluated using a Student's *t*-test. The significance was indicated as *, $p < 0.05$.

Table 1. Sequences of primers used

Gene	Forward (5'–3')	Reverse (5'–3')
MUC5AC	TGCACCCGGCATACAGCCATGCCC	GTTGCAGGCTCGTAGCAC
RPLPO	GGCGACCTGGAAGTCCAACT	CCATCAGCACCACAGCCTTC
HPRTI	GCCAGACTTTGTTGGATTTG	CTCTCATCTTAGGCTTTGTATTTTG

RESULTS

As detailed previously [27], three kinds of PLGA NPs were prepared according to an emulsion evaporation technique using various stabilizers, which allowed tuning NP surface charge. PLGA NPs exhibit a mean diameter in the range of 100–200 nm. All formulations have a narrow size distribution with a polydispersity index in the 0.1–0.2 range. Zeta potential measurements confirm that stabilizers influence NP surface charge: PLGA/CS NPs exhibit a positive zeta-potential (ζ = +32 ± 3 mV), whereas PLGA/PVA NPs are almost neutral (ζ = −5 ± 1 mV) and PLGA/PF68 NPs exhibit a negative zeta-potential (ζ = −24 ± 1 mV). Fluorescent NPs, obtained from Rhod-PLGA, showed the same surface properties.

Effect of nanoparticle surface properties on monolayer trans-epithelial resistance. Culturing Calu-3 cells at the air/liquid interface lead to formation of confluent monolayers which showed a gradual increase in TEER values due to the formation of tight junctions. The evaluation of the monolayer permeability through the TEER measurement has proven a good indicator of the integrity of this physical barrier [34]. Incubation of monolayers with PLGA/PVA NPs and PLGA/PF68 NPs at a subtoxic concentration of 200 $\mu g.mL^{-1}$, that has been shown to ensure at least 80% cell viability (Supplementary data, Fig. S1), did not alter the resistance of the epithelial layer. This was confirmed by the progressive increase over time of the TEER values without any significant difference compared to control cells. However, after exposure to PLGA/CS NPs, no significant increase of TEER was recorded during the 24 h of incubation (Fig. 1a). In order to precise TEER values upon exposure to PLGA/CS NPs, TEER was measured at several time points (Fig 1b). With respect to the initial value, a 20 % TEER decrease was already recorded after only 1 h of exposure to PLGA/CS NPs. The maximal reduction in TEER was recorded after 3 h exposure, with a 36% decrease compared to control cells. However, the decline in TEER was reversible and a progressive increase was then measured after 4 h of incubation despite the fact that the monolayers were still incubated with the PLGA/CS NPs.

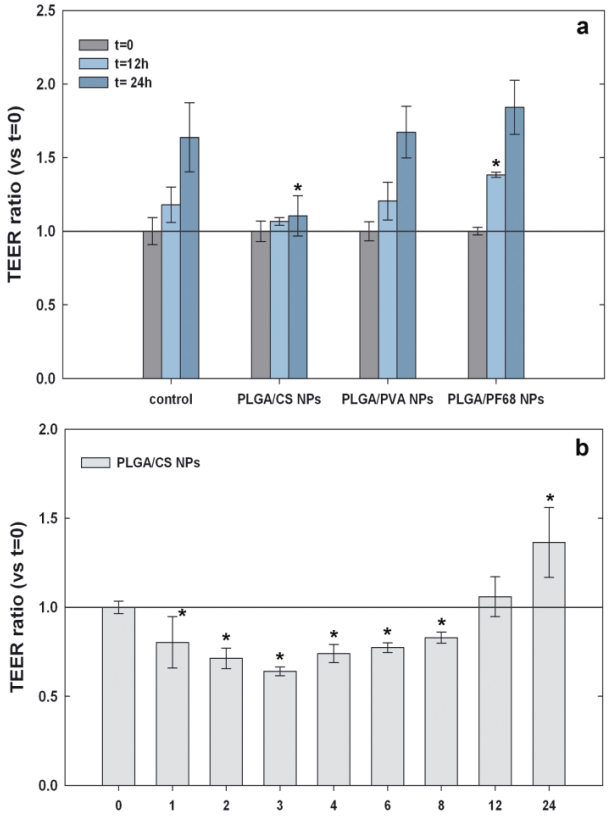

Figure 1. (a) Trans-epithelial electrical resistance (TEER) of Calu-3 cell monolayers following exposure to PLGA/CS, PLGA/PVA and PLGA/PF68 NPs. Untreated cells were used as control. (TEER was monitored at the beginning of exposure (t=0) and at t= 12 and 24 h). The significance was indicated as *, $p < 0.05$ (cells exposed to NPs vs control); (b) TEER values following exposure to PLGA/CS NPs. (TEER was monitored at the beginning of exposure (t=0) and at t= 1,2, 3, 4, 6, 8, 12 and 24 h). Results are expressed as TEER relative to the control mean value at t=0 and presented as mean ± SD (n = 3). The significance was indicated as *, $p < 0.05$ (cells exposed to PLGA/CS NPs vs untreated cells at t=0).

Cellular uptake of PLGA nanoparticles. Cellular uptake of NPs was evaluated by flow cytometry after incubation with each of the three kinds of fluorescent Rhod-PLGA NPs. A continuous fluorescence increase was observed over the course of the experiment (0-24 h) (Fig. 2). The effect of

NPs on cell autofluorescence was addressed using non-fluorescent NPs. Despite the difference of surface charge between NPs, the internalization profile of PLGA/PVA NPs and PLGA/CS NPs was similar. In contrast, the negatively charged PLGA/PF68 NPs were internalized in higher amounts. At 24 h, the fluorescence intensity obtained with PLGA/PF68 NPs was significantly higher compared to the values measured after exposure to PLGA/PVA NPs ($p < 0.05$) (Fig 3).

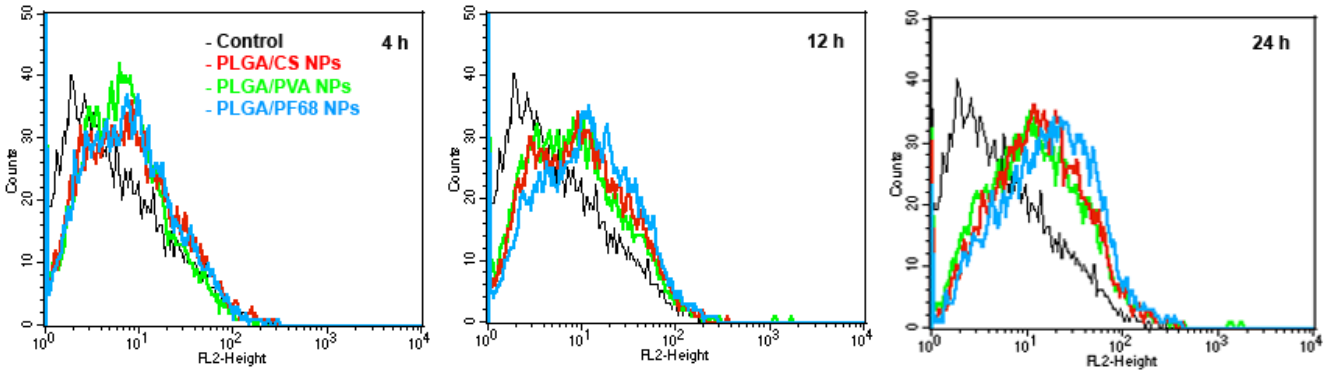

Figure 2. Fluorescence histogram profiles of Calu-3 cells at t= 4, 12 and 24 h following exposure to Rhod-PLGA/CS, Rhod-PLGA/PVA and Rhod-PLGA/PF68 NPs. The results were obtained after gating and selecting a fluorescence threshold. 10000 cells per sample were counted. Fig. 2. is representative of three independent experiments.

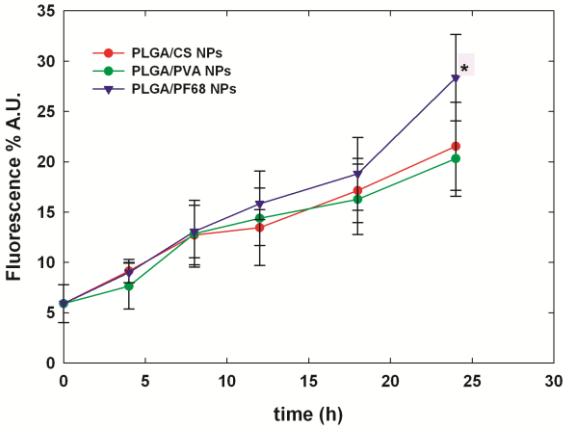

Figure 3. Cellular uptake of Rhod-PLGA/CS, Rhod-PLGA/PVA and Rhod-PLGA/PF68 NPs by Calu-3 cells Red fluorescence was measured at t = 4, 8, 12, 18 and 24 h. The results were obtained after gating and selecting a fluorescence threshold. 10000 cells per sample were counted. Data are expressed as mean ± SD (n = 3). * $p < 0.05$ (PLGA/PF68 NPs vs PLGA/PVA NPs).

Interaction of nanoparticles with the epithelium model. In order to investigate the penetration ability of the NPs, the cell-covering mucus layer was stained with the Alexafluor-488-labeled wheat germ agglutinin after 24 h of exposure to Rhod-PLGA NPs. Immediately after, the cell monolayers grown on Transwell® inserts and treated with the different NPs were imaged without fixing. For each Transwell® insert, the optical sections were processed in order to create an orthogonal view which allowed observing both the interaction of the NPs with the mucus and the diffusion in the depth of the cells after internalization (Fig. 4). The green fluorescence identifies the mucus which covers the cell surface, while the red fluorescent spots correspond to Rhod-PLGA NPs. The use of other dyes to stain the cell membrane, the nucleus or the cell volume was avoided in order to focus the attention only on the mucus and the NPs. The mucus being at the cell surface, the cells are located below the green fluorescent layer. For monolayers exposed to either PLGA/PVA NPs or PLGA/CS NPs, a yellow layer corresponding to the colocalization of mucus and NPs is visible in the upper part or the image demonstrating the interaction of NPs with the mucin chains and their partial entrapment,

thus limiting the amount of NPs able to diffuse inside the cells, as confirmed by the scarce red spots located in the cytoplasm. No significant differences could be observed between PLGA/PVA and PLGA/CS NPs. The behavior of the PLGA/PF68 NPs was completely different. At 24 h of incubation no NPs are visible in the mucus as revealed by the presence of two distinct layers: a green mucus layer at the cell surface and the layer of red spots inside the cells corresponding to the internalized Rhod-PLGA/PF68 NPs. NPs seem to diffuse unimpeded between mucin network, reach the surface of the epithelial monolayer before being internalized. These discrepancies in the NP behavior can also be clearly observed after 3D processing of the confocal microscopy images. Fig. S2 (See Supplementary Data) shows the presence of NPs entrapped into the mucus layer and their diffusion with subsequent cellular internalization.

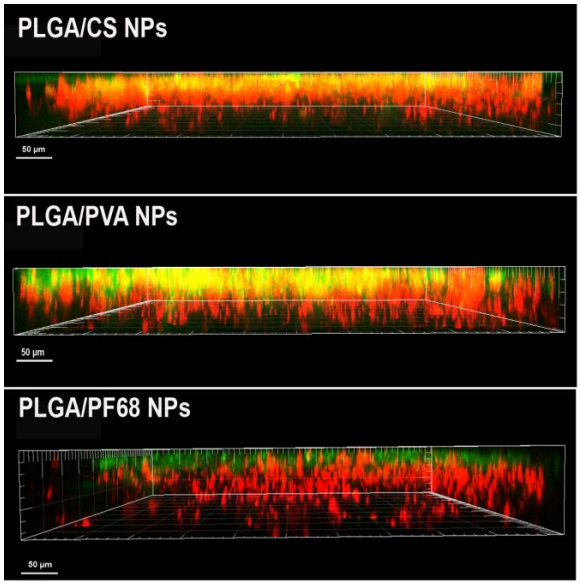

Figure 4. Orthogonal view (x,y plane) created from confocal laser microscopy sections of confluent Calu-3 monolayers exposed to Rhod-PLGA/CS, Rhod-PLGA/PVA and Rhod-PLGA/PF68 NPs for 24 h and subsequent staining of mucus with Alexafluor-488-labeled wheat germ agglutinin.

Influence of nanoparticle surface properties on MUC5AC gene expression and production. To investigate whether NPs could induce a harmful increase of mucus production, we measured MUC5AC content as a marker of mucus hypersecretion. Acrolein was chosen as a positive control. Acrolein was used at a subtoxic concentration (0.05 mM) which caused only a slight decrease of cell viability (94 ± 6 %) compared to untreated cells (Supplementary data, Fig. S3).

In order to quantify both the intracellular accumulation and the secretion of mucus at the cell surface, the amount of MUC5AC was measured by ELISA test in the cell lysates and in the monolayer mucus-containing-washing solutions, respectively. Results were expressed as a function of the intracellular total amount of protein. Exposure to NPs did not cause any variation of the MUC5AC intracellular content compared to the untreated cells. By contrast, an important increase of MUC5AC amount was observed following incubation with acrolein (Fig 5a). However, the amount of MUC5AC in the apical secretions accumulating over different periods of time was not modified after exposure to either NPs or acrolein (the MUC5AC concentration was comparable to the one measured for control cells) (Fig 5b).

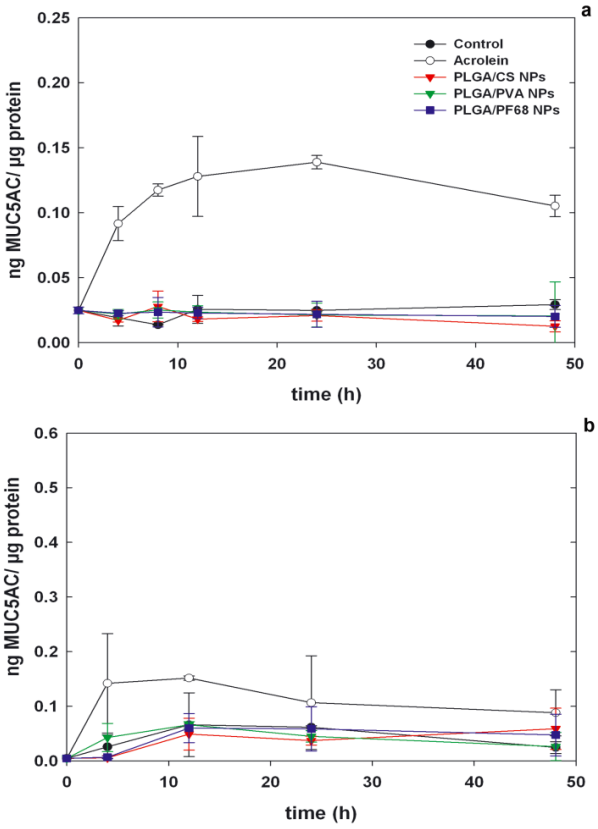

Figure 5. MUC5AC protein content in the cell lysates (a) and apical secretions accumulated in the monolayer washing solutions (b) after exposure to PLGA/CS, PLGA/PVA and PLGA/PF68 NPs. Untreated cells were used as control. Acrolein solution (0.05 mM) was used as a positive control. Data represent mean ± SD (n = 3).

Even if exposure to NPs did not increase MUC5AC production (both secreted and accumulated intracellularly), this observation did not exclude a possible activation of the signaling pathways involved in the control of the expression of the MUC5AC gene. Therefore, we investigated the MUC5AC gene expression at the transcriptional level by measuring mRNA levels after exposure to NPs compared to acrolein. No variation in MUC5AC mRNA level was recorded for the three kinds of NPs compared to the control over the course of the experiment (0-48 h) (Fig. 6). By contrast, a significant increase of MUC5AC gene expression was observed after 48 h exposure to acrolein. This is consistent with previous studies highlighting the irritant potential of this molecule [35-36].

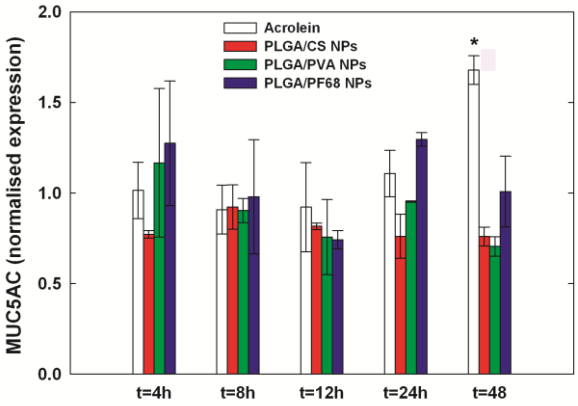

Figure 6. MUC5AC gene expression in Calu-3 cells after exposure to PLGA/CS, PLGA/PVA and PLGA/PF68 NPs. Acrolein (0.05 mM) was used as positive control. The data represent the levels of normalized expression in NPs-treated Calu-3 cells relative to control (untreated) cells and are reported as mean ± SD (n = 3). *$p < 0.05$ (acrolein-exposed vs untreated cells).

DISCUSSION

The tracheo-bronchial epithelial barrier constitutes the first defense of the organism against inhaled materials. The integrity of this barrier relies on the continuity of the superficial cell layer and the effectiveness of the adhesion between cells, mainly due to the formation of tight junctions. In addition, the layer of mucus at the cell surface contributes to the efficiency of this barrier, and could represent an obstacle to NP diffusion and interaction with underlying epithelial cells.

In this study, we have evaluated *in vitro* the influence of the physico-chemical properties of biodegradable NPs on their potential toxicity towards the bronchial airway barrier. The maintenance of the integrity of the airway epithelium is of pivotal importance for the defense of the organism against inhaled materials. The effect of NPs was investigated using the human bronchial Calu-3 cell line. These cells, cultured at the air/liquid interface, enable the formation of polarized tight monolayers and secrete mucus components which uniformly lie at the cell apical surface [37-38]. These

culture conditions thus provide an adequate *in vitro* model of the upper respiratory tract epithelial barrier.

Confluent monolayers were incubated with NPs and the integrity of the barrier was evaluated following acute exposure to NP displaying different physico-chemical properties. TEER measures the formation of occluding tight junctions and its value is an indicator of the epithelial permeability [34]. Decreases in TEER have been observed after exposure to tobacco smoke components as well as to manufactured NPs such as carbon nanotubes, and were assigned to the development of inflammatory reactions [39]. The consequent increase of permeability could have deleterious effects such as penetration of bacteria, viruses or other hazardous material.

Exposure to PLGA/PVA (neutral) NPs and PLGA/PF68 (negatively-charged) NPs did not cause any adverse effects on the epithelial barrier integrity since no significant differences were observed compared to the untreated cells. These results show that NPs do not interfere with the formation of complex interactions between the adhesion proteins involved in the formation of the tight junctions.

A different behavior was observed when cell monolayers were exposed to PLGA/CS (positively charged) NPs, which caused a decrease of TEER associated to an increase of the epithelial permeability. The ability of CS alone to open the tight junctions and to act as an absorption enhancer has been previously highlighted [40-43]. Our results suggest that the flexible CS moieties at the PLGA/CS NPs surface are able to interact with the tight junctions and affect their function due to the well known ability of CS to chelate the Ca^{2+} causing a decrease of its extracellular concentration [44]. Because of the fundamental role of the Ca^{2+} for the assembly of the tight junction proteins at the apical side of the cells, the calcium complexation affects the maintenance of the barrier integrity causing a drop in the epithelial resistance [45].

Destabilization occurred rapidly and a maximal reduction of TEER was recorded after three hours of incubation. Nevertheless, this effect was transient and reversible, as the TEER started to

increase until reaching the baseline value after 12 h of exposure. After 24 h, the epithelial barrier integrity was completely recovered and TEER value confirmed the formation of a stable impermeable monolayer. This reversible increase of the epithelial layer permeability opens up perspectives for the use of such PLGA/CS NPs for the systemic delivery of drugs after lung delivery. Interestingly, the rapid loss of epithelial integrity during the first hours of exposure was not associated to cell death. Indeed, as shown in our previous study, there was no reduction of cell viability following acute exposure to PLGA/CS NPs [27].

The mucus layer is known to provide an additional protection of the airway bronchial epithelium and its integrity is fundamental for the defense of the organism against inhaled exogenous materials. Our results suggest that the different NP surface properties induced a different interaction with the mucus layer which covers the cell surface, which in turn modified the internalization rate of the NPs.

On one hand, no significant differences could be observed in the interactions between PLGA/PVA or PLGA/CS NPs and the Calu-3 cells, after their application at the apical surface of the confluent monolayers cultured in the air/liquid conditions. Both these NPs are partially entrapped within the mucus which covers the monolayer surface. Regarding PLGA/CS NPs, CS is known to confer muco-adhesive properties to various NPs [46] by establishing electrostatic interactions between the amino groups of the CS and the negatively charged domains of the mucin chains which result from sialic acid and sulfated sugar molecules [47]. As a consequence of these interactions, some PLGA/CS NPs are entrapped in the network formed by the mucin chains which hold NPs back. Therefore, due to a slow diffusion rate of PLGA/CS NPs through the mucus layer, only a small amount of the applied NPs reach the cell surface and get internalized. Similar entrapment within the mucus layer has been observed for PLGA/PVA NPs and is probably due to the surface hydrophobicity of these NPs. Indeed, despite the PVA coating, the extent of Rose Bengal adsorption (data not shown)

showed a hydrophobic surface which allowed these NPs to interact with the hydrophobic domains of the mucin chains.

The orthogonal view of the cell monolayers observed by confocal microscopy confirms this behavior. The yellow layer corresponding to the colocalization of mucus and Rhod-PLGA highlights the entrapment of a certain amount of PLGA/CS and PLGA/PVA NPs. Translating these *in vitro* observations to the physiological *in vivo* situation, PLGA/PVA and PLGA/CS NPs would probably never interact with the underlying cells because of the muco-ciliary clearance function of the tracheobronchial airways which would sweep them off, before their internalization.

On the other hand, PLGA/PF68 NPs could rapidly diffuse in the mucin network and the total amount of internalized NPs at 24 h is significantly higher compared to PLGA/PVA NPs. The surface chemistry of the PLGA/PF68 NPs may be responsible for the faster diffusion rate and the highest percentage of cell associated fluorescence that corresponds to Rhod-PLGA NP internalization. Indeed, the presence of PF68 molecules confers a hydrophilic surface to these NPs which minimizes hydrophobic entrapment in the mucus. Moreover the low molecular weight of PF68 allows the mucoadhesion occurring *via* polymer interpenetration with mucus chains to be circumvented [23, 48-49]. The absence of a yellow layer on the top of the cell monolayer, in the confocal microscopy orthogonal view, confirms that the PLGA/PF68 NPs diffuse unimpeded and after 24 h, NPs were practically absent from the mucus layer.

Changes in density and quantity of mucus at the epithelial surface can be responsible of bronchial obstruction due to impaired muco-ciliary clearance and therefore compromise life. Among the different human MUC genes, the MUC5AC encodes the most secreted mucin by the tracheo-bronchial epithelial cells of both healthy individuals and patients with chronic lung diseases [50]. Moreover, MUC5AC is the most important mucin secreted by the Calu-3 cells. Therefore, we have first assessed the possible alteration of mucus production (turnover) and focused our attention both on the accumulation of the MUC5AC protein inside the cells and its possible secretion. Furthermore, we

have studied the potential effect of NPs on the gene expression. Noteworthy, exposure of confluent monolayers to NPs did not cause either an increased secretion of MUC5AC protein at the surface of the cell layer, nor an intracellular accumulation as observed by the quantification of MUC5AC protein in the washing solutions of the surface monolayer and in the cell lysate respectively. Furthermore, the MUC5AC mRNA levels were not changed by exposure to NPs, highlighting the absence of MUC5AC gene transcripts in the Calu-3 cells, regardless of NPs' surface chemistry and charge. Only the treatment with acrolein, which represents the most irritant component among the various constituents of the cigarette smoke [51], resulted in an increase of the MUC5AC gene expression and a higher production of the MUC5AC protein. These results thus confirmed the validity of the Calu-3 model to study deleterious effects towards the bronchial epithelium.

CONCLUSIONS

In conclusion, we have investigated the fundamental role of the physico-chemical surface properties of biodegradable PLGA NPs on their *in vitro* interactions with and potential toxicity towards a bronchial airway epithelial barrier model. Positively, negatively charged, as well as neutral PLGA NPs penetrate the mucus layer and get internalized by the underlying epithelial cells, although with significant differences. Negatively charged PLGA/PF68 NPs quickly diffuse unimpeded through the mucus layer and are highly internalized by the cells. Such NPs are thus valuable candidates for intracellular delivery of drugs to bronchial cells. In contrast, the mobility of PLGA/CS and PLGA/PVA NPs was reduced as consequence of interactions with the mucin chains. NPs do not cause alterations in TEER excepted for PLGA/CS NPs that were responsible for a transient and reversible opening of the tight junctions, which could allow application of these NPs for the systemic delivery of drugs due to their permeability-enhancing properties. Importantly, exposure to the three kinds of NPs does not promote the production of MUC5AC protein or the activation of the MUC5AC gene expression, thus confirming the absence of irritant action toward the bronchial epithelium. Taken

together, these *in vitro* results highlight the safety of biodegradable PLGA NPs towards the bronchial epithelial barrier, and the role of surface coating in the design of nanomedicine for local and systemic drug delivery.

ACKNOWLEDGMENTS

Authors would like to acknowledge M.N. Soler (Imagif Cell Biology Unit, Gif sur Yvette, France) for confocal microscopy experiments. This study was supported by ANSES ("Emerging risks" program) and by ANR (under reference 2009-CESA-011). S. Mura acknowledges the support of Univ. Paris-Sud and CNRS for her fellowship.

REFERENCES

1. Kumari, A.; Yadav, S. K.; Yadav, S. C., Biodegradable polymeric nanoparticles based drug delivery systems. *Colloids and Surfaces B: Biointerfaces* **2010,** 75, (1), 1-18.

2. Godin, B.; Sakamoto, J. H.; Serda, R. E.; Grattoni, A.; Bouamrani, A.; Ferrari, M., Emerging applications of nanomedicine for the diagnosis and treatment of cardiovascular diseases. *Trends in Pharmacological Sciences* **2010,** 31, (5), 199-205.

3. Pison, U.; Welte, T.; Giersig, M.; Groneberg, D. A., Nanomedicine for respiratory diseases. *European Journal of Pharmacology* **2006,** 533, (1-3), 341-350.

4. Sung, J. C.; Pulliam, B. L.; Edwards, D. A., Nanoparticles for drug delivery to the lungs. *Trends Biotechnol* **2007,** 25, (12), 563-70.

5. Patton, J. S.; Byron, P. R., Inhaling medicines: delivering drugs to the body through the lungs. *Nat Rev Drug Discov* **2007,** 6, (1), 67-74.

6. Yang, W.; Peters, J. I.; Williams, R. O., 3rd, Inhaled nanoparticles--a current review. *Int J Pharm* **2008,** 356, (1-2), 239-47.

7. Shoyele, S. A.; Cawthorne, S., Particle engineering techniques for inhaled biopharmaceuticals. *Advanced Drug Delivery Reviews* **2006,** 58, (9-10), 1009-1029.

8. Schneeberger, E. E.; Lynch, R. D., The tight junction: a multifunctional complex. *American Journal of Physiology - Cell Physiology* **2004,** 286, (6), C1213-28.

9. Chiba, H.; Osanai, M.; Murata, M.; Kojima, T.; Sawada, N., Transmembrane proteins of tight junctions. *Biochim Biophys Acta* **2008,** 1778, (3), 588-600.

10. Wan, H.; Winton, H. L.; Soeller, C.; Stewart, G. A.; Thompson, P. J.; Gruenert, D. C.; Cannell, M. B.; Garrod, D. R.; Robinson, C., Tight junction properties of the immortalized human bronchial epithelial cell lines Calu-3 and 16HBE14o. *Eur Respir J* **2000,** 15, (6), 1058-68.

11. Gonzalez-Mariscal, L.; Nava, P., Tight junctions, from tight intercellular seals to sophisticated protein complexes involved in drug delivery, pathogens interaction and cell proliferation. *Adv Drug Deliv Rev* **2005,** 57, (6), 811-4.

12. Stolnik, S.; Shakesheff, K., Formulations for delivery of therapeutic proteins. *Biotechnology Letters* **2009,** 31, (1), 1-11.

13. Knowles, M. R.; Boucher, R. C., Mucus clearance as a primary innate defense mechanism for mammalian airways. *J Clin Invest* **2002,** 109, (5), 571-7.

14. Cone, R. A., Barrier properties of mucus. *Advanced Drug Delivery Reviews* **2009,** 61, (2), 75-85.

15. Quraishi, M. S.; Jones, N. S.; Mason, J., The rheology of nasal mucus: a review. *Clin Otolaryngol Allied Sci* **1998,** 23, (5), 403-13.

16. Samet, J. M.; Cheng, P. W., The role of airway mucus in pulmonary toxicology. *Environ Health Perspect* **1994,** 102 Suppl 2, 89-103.

17. Groneberg, D. A.; Witt, C.; Wagner, U.; Chung, K. F.; Fischer, A., Fundamentals of pulmonary drug delivery. *Respir Med* **2003,** 97, (4), 382-7.

18. Evans, C. M.; Koo, J. S., Airway mucus: the good, the bad, the sticky. *Pharmacol Ther* **2009,** 121, (3), 332-48.

19. Jany, B.; Basbaum, C. B., Mucin in disease. Modification of mucin gene expression in airway disease. *American Review of Respiratory Disease* **1991,** 144, (3 Pt 2), S38-41.

20. Ling, S. H.; van Eeden, S. F., Particulate matter air pollution exposure: role in the development and exacerbation of chronic obstructive pulmonary disease. *International Journal of Chronic Obstructive Pulmonary Disease* **2009,** 4, 233-43.

21. Ahn, M. H.; Kang, C. M.; Park, C. S.; Park, S. J.; Rhim, T.; Yoon, P. O.; Chang, H. S.; Kim, S. H.; Kyono, H.; Kim, K. C., Titanium dioxide particle-induced goblet cell hyperplasia: association with mast cells and IL-13. *Respiratory Research* **2005,** 6, 34.

22. Haswell, L. E.; Hewitt, K.; Thorne, D.; Richter, A.; Gaça, M. D., Cigarette smoke total particulate matter increases mucous secreting cell numbers in vitro: A potential model of goblet cell hyperplasia. *Toxicology In Vitro* **2010,** 24, (3), 981-987.

23. Peracchia, M. T.; Harnisch, S.; Pinto-Alphandary, H.; Gulik, A.; Dedieu, J. C.; Desmaele, D.; d'Angelo, J.; Muller, R. H.; Couvreur, P., Visualization of in vitro protein-rejecting properties of PEGylated stealth polycyanoacrylate nanoparticles. *Biomaterials* **1999,** 20, (14), 1269-75.

24. Tang, B. C.; Dawson, M.; Lai, S. K.; Wang, Y. Y.; Suk, J. S.; Yang, M.; Zeitlin, P.; Boyle, M. P.; Fu, J.; Hanes, J., Biodegradable polymer nanoparticles that rapidly penetrate the human mucus barrier. *Proc Natl Acad Sci U S A* **2009,** 106, (46), 19268-73.

25. Yang, M.; Lai, S. K.; Wang, Y. Y.; Zhong, W.; Happe, C.; Zhang, M.; Fu, J.; Hanes, J., Biodegradable nanoparticles composed entirely of safe materials that rapidly penetrate human mucus. *Angewandte Chemie. International Edition in English* **2011,** 50, (11), 2597-600.

26. Suk, J. S.; Lai, S. K.; Wang, Y. Y.; Ensign, L. M.; Zeitlin, P. L.; Boyle, M. P.; Hanes, J., The penetration of fresh undiluted sputum expectorated by cystic fibrosis patients by non-adhesive polymer nanoparticles. *Biomaterials* **2009,** 30, (13), 2591-7.

27. Mura, S.; Hillaireau, H.; Nicolas, J.; Le Droumaguet, B.; Marsaud, V.; Guetin, C.; Zanna, S.; Tsapis, N.; Fattal, E., Surface properties do not affect the in vitro toxicity of biodegradable nanoparticles towards bronchial cells. *Submitted* **2011**.

28. Shive, M. S.; Anderson, J. M., Biodegradation and biocompatibility of PLA and PLGA microspheres. *Adv Drug Deliv Rev* **1997,** 28, (1), 5-24.

29. Anderson, J. M., In vivo biocompatibility of implantable delivery systems and biomaterials. *Eur J Pharm Biopharm* **1994,** 40, 1-8.

30. Gómez-Gaete, C.; Fattal, E.; Silva, L.; Besnard, M.; Tsapis, N., Dexamethasone acetate encapsulation into Trojan particles. *Journal of Controlled Release* **2008,** 128, (1), 41-49.

31. Geys, J.; Nemery, B.; Moreno, E. A.; Hoet, P. H., Cytotoxicity of SiO2 in A549 cells. *Toxicol Appl Pharmacol* **2007,** 220, (2), 225; author reply 226.

32. Gomez-Gaete, C.; Tsapis, N.; Besnard, M.; Bochot, A.; Fattal, E., Encapsulation of dexamethasone into biodegradable polymeric nanoparticles. *Int J Pharm* **2007,** 331, (2), 153-9.

33. Vandesompele, J.; De Preter, K.; Pattyn, F.; Poppe, B.; Van Roy, N.; De Paepe, A.; Speleman, F., Accurate normalization of real-time quantitative RT-PCR data by geometric averaging of multiple internal control genes. *Genome Biology* **2002,** 3, (7), RESEARCH0034.

34. Florea, B. I.; Cassara, M. L.; Junginger, H. E.; Borchard, G., Drug transport and metabolism characteristics of the human airway epithelial cell line Calu-3. *J Control Release* **2003,** 87, (1-3), 131-8.

35. Chen, Y. J.; Chen, P.; Wang, H. X.; Wang, T.; Chen, L.; Wang, X.; Sun, B. B.; Liu, D. S.; Xu, D.; An, J.; Wen, F. Q., Simvastatin attenuates acrolein-induced mucin production in rats: involvement of the Ras/extracellular signal-regulated kinase pathway. *International Immunopharmacology* **2010,** 10, (6), 685-93.

36. Haswell, L. E.; Hewitt, K.; Thorne, D.; Richter, A.; Gaca, M. D., Cigarette smoke total particulate matter increases mucous secreting cell numbers in vitro: a potential model of goblet cell hyperplasia. *Toxicol In Vitro* **2010,** 24, (3), 981-7.

37. Fiegel, J.; Ehrhardt, C.; Schaefer, U. F.; Lehr, C. M.; Hanes, J., Large porous particle impingement on lung epithelial cell monolayers--toward improved particle characterization in the lung. *Pharm Res* **2003,** 20, (5), 788-96.

38. Grainger, C. I.; Greenwell, L. L.; Lockley, D. J.; Martin, G. P.; Forbes, B., Culture of Calu-3 cells at the air interface provides a representative model of the airway epithelial barrier. *Pharm Res* **2006,** 23, (7), 1482-90.

39. Balharry, D.; Sexton, K.; BeruBe, K. A., An in vitro approach to assess the toxicity of inhaled tobacco smoke components: nicotine, cadmium, formaldehyde and urethane. *Toxicology* **2008,** 244, (1), 66-76.

40. Illum, L., Chitosan and its use as a pharmaceutical excipient. *Pharm Res* **1998,** 15, (9), 1326-31.

41. Artursson, P.; Lindmark, T.; Davis, S. S.; Illum, L., Effect of chitosan on the permeability of monolayers of intestinal epithelial cells (Caco-2). *Pharm Res* **1994,** 11, (9), 1358-61.

42. Fernandez-Urrusuno, R.; Calvo, P.; Remunan-Lopez, C.; Vila-Jato, J. L.; Alonso, M. J., Enhancement of nasal absorption of insulin using chitosan nanoparticles. *Pharm Res* **1999,** 16, (10), 1576-81.

43. Janes, K. A.; Calvo, P.; Alonso, M. J., Polysaccharide colloidal particles as delivery systems for macromolecules. *Adv Drug Deliv Rev* **2001,** 47, (1), 83-97.

44. Bravo-Osuna, I.; Millotti, G.; Vauthier, C.; Ponchel, G., In vitro evaluation of calcium binding capacity of chitosan and thiolated chitosan poly(isobutyl cyanoacrylate) core-shell nanoparticles. *Int J Pharm* **2007,** 338, (1-2), 284-90.

45. Ma, T. Y.; Tran, D.; Hoa, N.; Nguyen, D.; Merryfield, M.; Tarnawski, A., Mechanism of extracellular calcium regulation of intestinal epithelial tight junction permeability: role of cytoskeletal involvement. *Microscopy Research and Technique* **2000,** 51, (2), 156-68.

46. Sogias, I. A.; Williams, A. C.; Khutoryanskiy, V. V., Why is chitosan mucoadhesive? *Biomacromolecules* **2008,** 9, (7), 1837-42.

47. Lai, S. K.; Wang, Y. Y.; Hida, K.; Cone, R.; Hanes, J., Nanoparticles reveal that human cervicovaginal mucus is riddled with pores larger than viruses. *Proc Natl Acad Sci U S A* **2010,** 107, (2), 598-603.

48. Lai, S. K.; Wang, Y.-Y.; Hanes, J., Mucus-penetrating nanoparticles for drug and gene delivery to mucosal tissues. *Advanced Drug Delivery Reviews* **2009,** 61, (2), 158-171.

49. Gref, R.; Luck, M.; Quellec, P.; Marchand, M.; Dellacherie, E.; Harnisch, S.; Blunk, T.; Muller, R. H., 'Stealth' corona-core nanoparticles surface modified by polyethylene glycol (PEG): influences of the corona (PEG chain length and surface density) and of the core composition on phagocytic uptake and plasma protein adsorption. *Colloids Surf B Biointerfaces* **2000,** 18, (3-4), 301-313.

50. Hovenberg, H. W.; Davies, J. R.; Herrmann, A.; Linden, C. J.; Carlstedt, I., MUC5AC, but not MUC2, is a prominent mucin in respiratory secretions. *Glycoconjugate Journal* **1996,** 13, (5), 839-47.

51. Fowles, J.; Dybing, E., Application of toxicological risk assessment principles to the chemical constituents of cigarette smoke. *Tobacco Control* **2003,** 12, (4), 424-430.